

# Evaluation of a Three-Dimensional Mathematical Model of a Power Station Boiler

P. J. Coelho  
Assistant Professor.

M. G. Carvalho  
Professor.

Mechanical Engineering Department,  
Instituto Superior Técnico,  
Technical University of Lisbon,  
Av. Rovisco Pais,  
1096 Lisboa Codex,  
Portugal

*A three-dimensional mathematical model based on the numerical solution of the governing equations of mass, momentum, and energy, and transport equations of scalar quantities is presented. The model is applied to a power station boiler of the Portuguese Electricity Utility for which experimental data are available. Predictions of the gas temperature and chemical species concentrations are compared with the measurements. Three different grids were employed to ensure that conclusions are not affected by the grid refinement. It was found that using a combustion model based on the chemical equilibrium assumption, the predicted gas species concentrations are in good agreement with the data and the temperature profiles display the correct trend, although the temperature was underpredicted, especially in the burner region. The influence of the air/fuel ratio and power load were also successfully simulated. The present results reveal the predictive capabilities of the model and its usefulness for design or optimization studies.*

## 1 Introduction

In power station boilers, a significant amount of fossil fuels is consumed. The limited sources of these fuels and their uneven distribution over the world will tend to increase the price of the fuels with time. This trend is accentuated by increased energy demand. Therefore, there is a need to improve combustion efficiency and to reduce fuel consumption. This motivates the search for new fuel resources and the burning of fuels of lower quality. But these fuels generally yield more pollutants. To face the increasingly more restrictive emission regulations, improved combustion strategies and burner designs are required. In addition, the foregoing requirements should not adversely affect the investment and operation costs and the lifetime of the equipment. Experimental techniques and computational methods are two complementary tools that may help engineers meet all these requirements.

Only a few experimental studies have been performed in full-scale utility boilers. This is due to the difficulties involved, namely the limited physical access to data and the harsh environment. Consequently, the experiments require skill and time and become very expensive. Moreover, they are subject to inaccuracy. Most of them have been performed in boilers with a power output below 80 MWe (see Butler and Webb, 1991). Recently, Cassiano et al. (1994) carried out experimental work in a 250 MWe power station boiler of the Portuguese Electricity Utility. The results are used in the present numerical study for evaluation of the mathematical model.

The mathematical modeling of utility boilers based on the solution of the three-dimensional governing equations for mass, momentum, energy, and other scalar variables has only recently been attempted. Although most of the numerical techniques and physical models were developed about two decades ago, the first numerical study of this kind applied to utility boilers was reported by Robinson (1985). He applied the model to a tangentially fired gaseous furnace and compared the predicted gas temperatures and heat fluxes with experimental data acquired on two large furnaces. Thereafter, several studies have been published in the literature.

Abbas and Lockwood (1986) and Lockwood et al. (1988) studied two power station boilers, one front-wall fired and the other corner-fired. Comparison with measurements was restricted to isothermal velocity data collected in a scale model. A similar study was reported by Sargianos et al. (1990), who simulated the isothermal air flow in a laboratory-scale boiler model and methane combustion in a large utility boiler. The isothermal air flow predictions in the scale model showed qualitative trends aligned with certain preliminary measurements. Carvalho and Coelho (1990) applied a three-dimensional model to an oil-fired water tube boiler where a few heat flux measurements were available. The calculated fluxes were in good agreement with the observed ones. Bonvini et al. (1991) applied a similar model to the prediction of NO<sub>x</sub> emissions from a large utility boiler furnace. Comparison with experimental measurements was limited to average concentration at the furnace outlet. All these works report applications to gas or oil-fired boilers, but other studies in coal-fired boilers have also been performed (Boy and Kent, 1986; Görner and Zinser, 1988; Fiveland and Wessel, 1988; Fiveland and Latham, 1991; Luo et al., 1991; Epple and Schnell, 1992; Coimbra et al., 1994). The evaluation of the mathematical models used in the studies mentioned above is limited by the scarceness of available data.

The present paper describes the application of a mathematical model to a power station boiler of the Portuguese Electricity Utility. Preliminary calculations for standard operating conditions were presented previously (Carvalho et al., 1991) as was a comparative study of the performance of the boiler for fuel oil and natural gas firing (Carvalho et al., 1990). An analysis of the heat transfer phenomena with emphasis on the influence of the uncertainties in the wall temperature and emissivity distributions on the predicted heat transfer was also performed (Coelho and Carvalho, 1992). In these previous works only predicted results were presented, since experimental measurements were not available. Recently, an experimental study was carried out in this boiler. The main objective of the present paper is to report the evaluation of the model by means of comparison of the predicted results with the measurements obtained. These include operation at two different air/fuel ratios and power loads. Due to the limited data available in utility boilers, this study represents an important contribution to the evaluation of current three-dimensional mathematical models.

The mathematical model is presented in the next section. In section 3 the modeled boiler is described, and in section 4 some

Contributed by the International Gas Turbine Institute for publication in the JOURNAL OF ENGINEERING FOR GAS TURBINES AND POWER. Manuscript received by the International Gas Turbine Institute June 23, 1993; revision received April 4, 1996. Associate Technical Editor: H. L. Julien.

numerical details of the computations are provided. The results are presented and discussed in section 5. The main conclusions are drawn in the last section.

## 2 Mathematical Model

The mathematical model is based on the numerical solution of the conservation equations for mass, momentum, and energy, and transport equations for scalar variables. All these equations may be cast in the following general form:

$$\frac{\partial}{\partial x_j} (\rho \tilde{u}_j \phi) = \frac{\partial}{\partial x_j} \left( \Gamma_\phi \frac{\partial \phi}{\partial x_j} - \rho \tilde{u}_j'' \phi'' \right) + \bar{\rho} \tilde{S}_\phi \quad (1)$$

where  $\phi$  is the dependent variable;  $u_j$ , the Cartesian velocity component along direction  $x_j$ ;  $\rho$ , the density;  $\Gamma_\phi$ , the diffusion coefficient; and  $S_\phi$ , the source term.

Equation (1) stands for the mass conservation equation when  $\phi = 1$ ; the momentum conservation equation when  $\phi$  is a velocity component; the energy conservation equation when  $\phi$  is the stagnation enthalpy; or the transport equation of a scalar when  $\phi$  is a scalar variable, such as mixture fraction.

To close Eq. (1) the Reynolds stresses  $\tilde{u}_i'' \tilde{u}_j''$  and the turbulent scalar fluxes  $\tilde{u}_i'' \phi''$  should be expressed in terms of known quantities. The  $k-\epsilon$  turbulent viscosity/diffusivity model has generally been employed for that purpose in the mathematical modeling of utility boilers and it was also used in the present work. It assumes a linear relationship between the Reynolds stresses and the rate of strain:

$$-\bar{\rho} \tilde{u}_i'' \tilde{u}_j'' = \mu_t \left( \frac{\partial \tilde{u}_i}{\partial x_j} + \frac{\partial \tilde{u}_j}{\partial x_i} \right) - \frac{2}{3} \left( \bar{\rho} k + \mu_t \frac{\partial \tilde{u}_k}{\partial x_k} \right) \delta_{ij} \quad (2)$$

and a gradient diffusion hypothesis for the calculation of the turbulent scalar fluxes:

$$-\bar{\rho} \tilde{u}_i'' \phi'' = \frac{\mu_t}{\sigma_\phi} \frac{\partial \phi}{\partial x_i} \quad (3)$$

In these expressions it is assumed that the approximations used for constant density flows remain valid without explicitly accounting for density fluctuations (see Jones and Whitelaw, 1982). The solution of transport equations for the turbulent kinetic energy,  $k$ , and its dissipation rate,  $\epsilon$ , allow the calculation of the turbulent viscosity  $\mu_t$  ( $\mu_t = C_\mu \rho k^2 / \epsilon$ ). Standard values were assigned to all the constants of the model (Launder and Spalding, 1974).

The density is calculated from the pressure, temperature, and chemical gas composition using the equation of state for a perfect gas. The temperature is related to the enthalpy by a well-known thermodynamic relationship. The calculation of the chemical gas composition requires a combustion model.

The combustion model assumes that the reaction rates are high enough that the chemical reactions take place instantaneously as soon as the reactants are brought together. Combustion

is controlled by mixing rather than kinetic phenomena. Therefore, the instantaneous thermochemical state of the gaseous mixture depends only upon strictly conserved scalar variables. All these variables are linearly related when it is further assumed that the system is adiabatic and the mass diffusion coefficients of all the chemical species and the thermal diffusion coefficient are equal. In such a case, the mixture fraction is often taken as the dependent variable. The instantaneous values of the mass fractions of all chemical species, temperature, and density may be found from the instantaneous value of the mixture fraction.

The relation between the gas composition and the mixture fraction depends on the model employed. In this work two different models were used. In the chemical equilibrium model, which was used in most of the cases, it is assumed that chemical equilibrium prevails and the instantaneous gas composition is calculated from the minimization of the free Gibbs energy, following Gordon and McBride (1971). Complete chemical equilibrium was assumed for values of mixture fraction,  $f$ , smaller than a threshold value,  $f_c$ , and frozen mixing (adiabatic mixing of mixtures at  $f = f_c$  and  $f = 1$ ) was assumed for  $f > f_c$ . The threshold value  $f_c$  was selected to match the peak measured CO concentration. The values of the instantaneous mass fractions of the chemical species as a function of the mixture fraction are stored in a look-up table. In the simple chemically reacting system (SCRS) model it is supposed that combustion takes place as a single-step irreversible reaction, where the fuel and the oxidant react instantaneously, yielding combustion products. This assumption yields piecewise linear relationships between the instantaneous mass fractions of oxygen, fuel, nitrogen, products, and the mixture fraction (see, e.g., Lockwood and Naguib, 1975).

In utility boilers a significant proportion of the heat released in combustion is transferred to the walls and it is not correct to consider the combustion chamber as adiabatic. Hence, the enthalpy is not linearly related to the mixture fraction and an additional assumption on how these variables are related is needed. Here, a piecewise linear relationship as suggested by Abou-Ellail et al. (1978) was used. The temperature can be determined from the enthalpy using well-known thermodynamic relations and the density is obtained from the ideal gas equation of state.

Due to the turbulent nature of the flow, mixture fraction fluctuations should be taken into account to calculate the mean values of the mass fractions, density and temperature. This was accomplished by prescribing a clipped Gaussian shape for the mixture fraction probability density function (Lockwood and Naguib, 1975). Hence, density weighted and nonweighted mean values are calculated as:

$$\bar{\phi} = \int_0^1 \phi(f) p(f) df \quad (4)$$

$$\bar{\phi} = \bar{\rho} \int_0^1 \frac{\phi(f)}{\rho(f)} p(f) df \quad (5)$$

## Nomenclature

$C_\mu$  = constant of  $k-\epsilon$  turbulence model  
 $k$  = turbulent kinetic energy  
 $p$  = pressure  
 $p(f)$  = probability density function  
 $S_\phi$  = source term of the discretized  $\phi$  equation  
 $u_i$  = velocity component along  $i$  direction  
 $x_i$  = Cartesian coordinate in  $i$  direction

$\Gamma_\phi$  = diffusion coefficient of variable  $\phi$   
 $\delta_{ij}$  = Kronecker tensor  
 $\epsilon$  = dissipation rate of turbulent kinetic energy  
 $\phi$  = dependent variable in a transport equation  
 $\mu$  = dynamic viscosity  
 $\rho$  = density  
 $\sigma_\phi$  = Prandtl/Schmidt number of variable  $\phi$

## Subscripts

$i$  = spatial direction  
 $t$  = turbulent  
 $\phi$  = dependent variable

## Superscripts

$\bar{\quad}$  = Reynolds-averaged value  
 $\tilde{\quad}$  = Favre-averaged value  
 $\prime\prime$  = fluctuation quantity in Favre-averaging

The probability density function is specified by the mean value and variance of the mixture fraction. Transport equations are solved for these two quantities.

The radiative heat transfer plays a dominant role in utility boilers and enters in the energy conservation equation as a source term. Here, it was calculated by means of the discrete transfer model (Lockwood and Shah, 1981), which is based on the solution of the radiative heat transfer equation along specified directions. In this model, the temperature and the absorption coefficient of the medium are assumed to be constant in each control volume resulting from the discretization of the physical domain. For all the control volumes adjacent to the boundary, the central points of the faces of the control volumes coincident to the boundary are determined. Let  $P$  be one such point. The hemisphere centered in  $P$  is discretized into a given number of solid angles. Each solid angle defines a direction along which radiation beams are fired and the radiative heat transfer equation is solved. Hence, given a point  $P$  at the center of a cell face on the boundary, a radiation beam is fired from  $P$  for each one of the directions selected above. The path of a radiation beam is followed until it hits another boundary. Let  $Q_i$  be the impingement point. Although, in general,  $Q_i$  is not the central point of a boundary cell, it is assumed that the radiation intensities at  $Q_i$  and at the central point of the cell that contains  $Q_i$  are equal. The radiation intensity leaving that cell is either known or guessed from a previous iteration. Then, starting from  $Q_i$ , the path of the beam is followed back to the origin (point  $P$ ), and the radiative transfer equation is integrated analytically along this path, allowing the calculation of the radiation intensity arriving at point  $P$ . The incident radiative heat flux at point  $P$  is calculated by adding the contributions due to all the radiation beams that reach point  $P$ , i.e., from all the directions resulting from the discretization of the hemisphere centered in  $P$ . This procedure is repeated for all the cell faces on the boundary. Then, the boundary conditions (prescribed temperature in the present study) are applied. This allows for an improved guess of the radiosity at the boundary. The iterative procedure continues until the convergence criterion is satisfied.

The source term of the energy equation in each control volume is obtained by the summation of the change of radiation intensity within the control volume for all the rays that cross it. Additional details of the method are given by Lockwood and Shah (1981).

Scattering of the participating medium was neglected. This is a good assumption for gas or oil-fired boilers. The absorption coefficient of the medium is calculated from the emissivity of the gas/soot mixture. The emissivity is calculated using the two grey plus one clear gas approach of Hottel and Sarofim (1967) extended to account for soot. The coefficients determined by Truelove (1976) were used. Soot concentration was predicted using the soot formation model of Khan and Greeves (1974) and the soot oxidation model of Magnussen and Hjertager (1977).

The governing equations are integrated over each control volume and discretized using finite differences. The central differences scheme is employed for all but convective terms, which are discretized using the hybrid central differences/upwind scheme. The solution algorithm is based on the SIMPLE method. The sets of discretized equations are solved using the Gauss-Seidel line-by-line iteration procedure.

### 3 The Modelled Boiler

The mathematical and physical models described in the previous section were applied to a boiler of the Portuguese Electricity Utility, schematically shown in Fig. 1(a). It is a natural circulation drum boiler with a pressurized combustion chamber, two parallel passages by the convection zone and superheating. The walls of the combustion chamber, the vaporization panels, are vertical welded tubes. Water circulates in these tubes and partly

vaporizes due to the heat released in the combustion chamber, which is transferred to the walls. The boiler is fired from three levels with four oil burners in each level, as shown in Fig. 1(b). A detail of the burners is presented in Fig. 1(c).

At maximum capacity the boiler produces 771 ton/h of steam at 167 bar and 545°C. The operating conditions are those for which experimental data are available, as summarized in Table 1. Case 1 corresponds to the standard operating conditions at full load (250 MWe). In case 2 the air/fuel ratio was reduced but the power load is the same, whereas in case 3 the boiler is operating at partial load. The fuel oil properties are given in Table 2.

The present model was applied to the combustion chamber whose overall dimensions are  $8.57 \times 11.43 \times 19.96$  m<sup>3</sup> along the  $x$ ,  $y$ , and  $z$  directions, respectively. The simplified combustion chamber geometry is presented in Fig. 1(b). Due to the symmetry, only one half was modeled. Figure 1(b) also shows the inspection ports, which provide access for the probes.

Experimental work was recently carried out in this boiler (Cassiano et al., 1994). Gas temperatures were measured using a 3.5-m-long, double-shielded, water-cooled suction pyrometer, which consists of a Pt/Pt-13 percent Rh thermocouple of 350  $\mu$ m diameter protected by radiation shields from losses to the combustion chamber walls. Major gas species concentrations were obtained by a gas sampling probe connected to gas analyzers. The probe consists of a sampling tube of 2 mm diameter mounted in a water-cooled jacket of 50 mm diameter and 3.5 m length. According to Cassiano et al. (1994) it is expected that the measured gas species concentrations are close to the density-weighted averages within 10 percent of the maximum measured value.

### 4 Numerical Details

The fuel oil is atomized in each burner and enters the combustion chamber as a spray. In the present model it is assumed that the droplets vaporize instantaneously and only the gas-phase flow is considered. The wall temperature and emissivity were taken as 700 K and 0.65, respectively, which is expected to be a good assumption. In fact, a previous sensitivity study (Coelho and Carvalho, 1992), where a coupling algorithm between the physical phenomena occurring in the combustion chamber and in the water wall tubes was proposed, showed that the influence of the wall temperature distribution on the predictions is negligible. Moreover, it was shown that the heat transfer phenomena are influenced by the wall emissivity but the gas temperature and composition are only marginally affected, provided that the wall emissivity is not too different from the actual one.

Calculations were performed using a mesh with  $16 \times 34 \times 60$  grid nodes along the  $x$ ,  $y$ , and  $z$  directions, respectively (see Fig. 2(a)). Hereafter, this grid will be called grid 1. The grid is very fine in the burner region where neighboring grid lines are undistinguishable. Therefore, a detail of the grid is shown in Fig. 2(b). In this figure the dashed lines are the faces of the control volumes and the solid lines identify the boundaries of the fuel inlet, atomizing air inlet, divider wall, and combustion air inlet. A coarser grid was employed for the calculation of radiative heat transfer comprising  $10 \times 9 \times 20$  grid nodes. This allows savings in CPU time without adverse effects on the solution accuracy (see, e.g., Abbas and Lockwood, 1986). Additional savings were achieved by calling the radiation subroutines only every 10 iterations. Hence, the converged solution, achieved when the sum of the normalized absolute residuals of each dependent variable decreased to values below  $2 \times 10^{-3}$ , is obtained in about 1000 iterations and 6 hours CPU time (VAX 9000-440).

Two other meshes were employed to evaluate the influence of grid refinement on numerical accuracy. It would be desirable to duplicate the number of grid nodes in each direction since this would allow the use of Richardson extrapolation to estimate

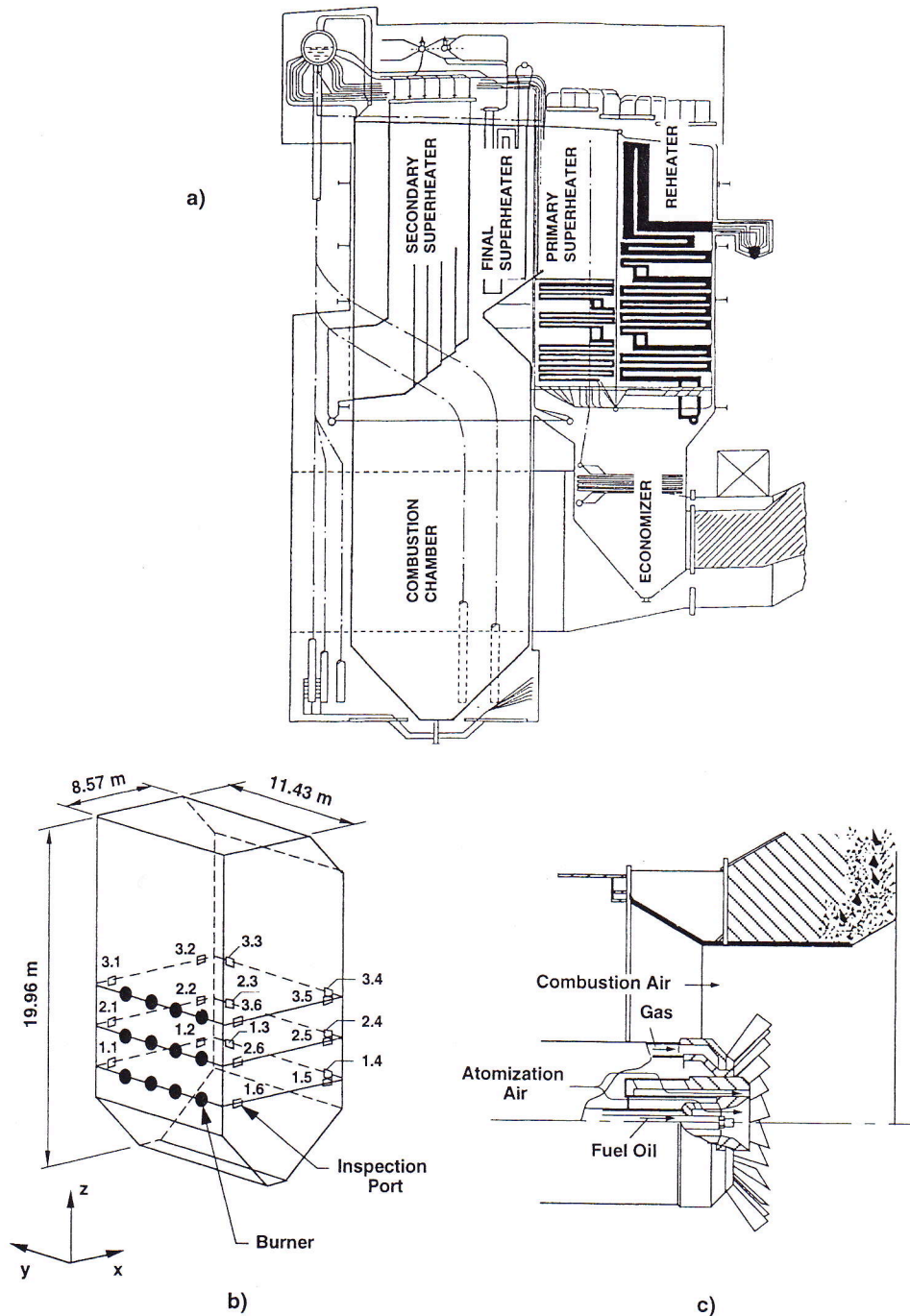


Fig. 1 (a) Sketch of the power station boiler; (b) simplified geometry of the combustion chamber with identification of the burners and inspection ports; (c) detail of a burner

the solution error. However, this would require many grid nodes and several days of CPU time. Therefore, a compromise solution was sought in which the grid was refined only either along the  $y$  and  $z$  directions or along the  $x$  direction. Hence, additional computations were carried out using grid 2 ( $16 \times 54 \times 98$  grid nodes) and grid 3 ( $32 \times 34 \times 60$  grid nodes).

## 5 Results and Discussion

**5.1 Standard Operating Conditions.** Figures 3(a), 3(b), and 3(c) show the predicted velocity component along the  $x$  direction, temperature, and mixture fraction profiles along the axis of the top level burner, close to the side wall. The profiles obtained using the three grids mentioned above are

plotted. These profiles were selected to illustrate the grid dependency. It can be seen that the three grid schemes yield qualitatively similar predicted profiles. However, significant differences may be found between the numerical solutions at certain locations. For example, the predicted  $u$  velocity at  $x = 4.3$  m is about 10 m/s higher for grid 3 than for grids 1 and 2. The temperature and mixture fraction profiles are similar for the three grids and exhibit steep gradients near the burner. The calculations performed using grid 3, which has twice as many grid nodes along the  $x$  direction as grids 1 and 2, reveal a higher fuel consumption rate for  $x$  values up to  $x \approx 1.3$  m and a smaller consumption rate further downstream up to  $x \approx 4.0$  m.

Therefore, the predicted results cannot be regarded as completely grid independent. This conclusion is consistent with the

Table 1 Operating conditions

Case	1	2	3
Load (MWe)	250	250	125
Air mass flow rate (ton/h)	805	769	459.3
Fuel mass flow rate (ton/h)	52.7	52.7	28.8
O <sub>2</sub> volumetric concentration in flue gases (%)	1.5	0.75	3.0
Inlet air temperature (°C)	335	343	290

Table 2 Fuel-oil properties

Composition (average)	Carbon:	86.52%	
	Hydrogen:	11.06%	
	Nitrogen:	0.72%	
	Sulfur:	2.08%	(ASTM D129)
Heating Value		10076 kcal/kg	(ASTM D129)

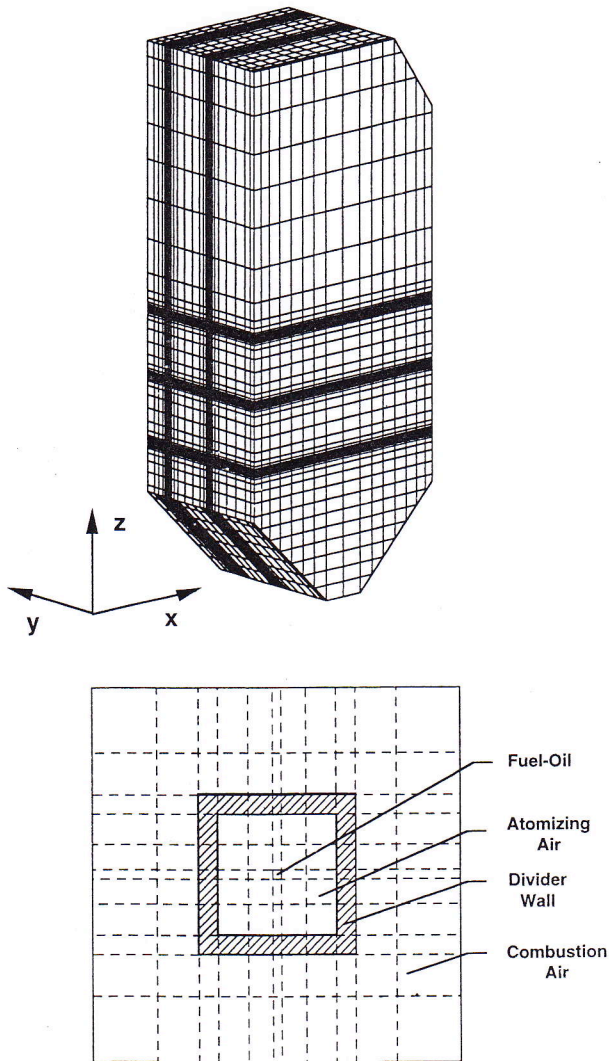


Fig. 2 (a) Computational grid (16 × 34 × 60 grid nodes); (b) detail of the grid in the burners region

one of Gillis and Smith (1990), who have found that the calculation of an isothermal flow in a pilot scale wall-fired furnace requires more than 250,000 grid nodes. So, the comparison presented below between the predictions and the data for the

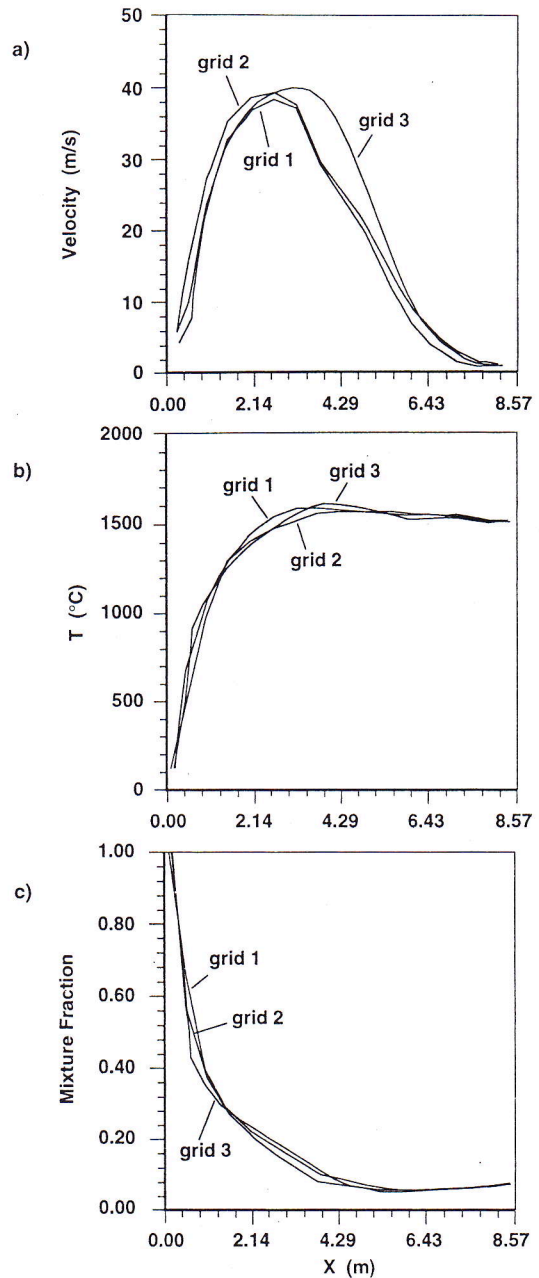


Fig. 3 Predicted velocity, temperature, and mixture fraction profiles along the axis of the top level burner close to the side walls (grid 1: 16 × 34 × 60; grid 2: 16 × 54 × 98; grid 3: 32 × 34 × 60)

boiler analyzed here includes consideration of the numerical solutions obtained for the three grids. This enables one to find out whether discrepancies may be attributed to grid refinement or not.

The comparison between predicted and measured temperature profiles along the axis of inspection ports 1.5 and 3.6 is illustrated in Fig. 4. Close to the back wall and just above the ash pit (inspection port 1.5; see Fig. 1(b)) the predicted temperature profile is relatively flat and nearly grid independent. However, the temperature is underpredicted by 50° to 150°C. The agreement between the three different numerical solutions suggests that this discrepancy is due to the modeling assumptions rather than numerical reasons. Since this profile is in a region where the fuel has already been consumed, the mixture fraction fluctuations are negligible. Therefore, the underprediction of temperature reveals an overprediction of the radiation loss. This suggests that the absorption coefficient was overesti-

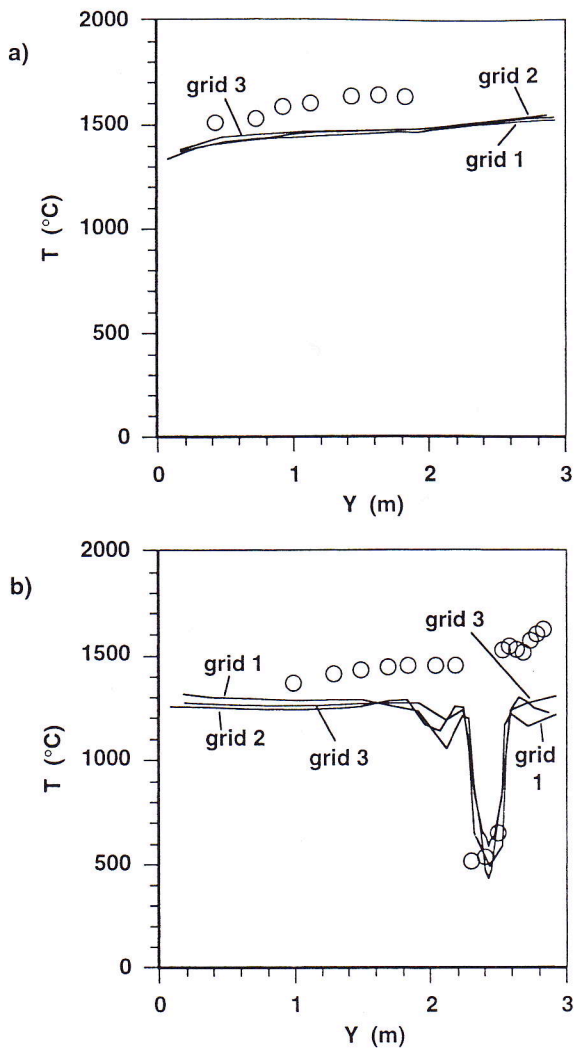


Fig. 4 Comparison between predicted (solid lines) and measured (symbols) temperature profiles: (a) profile along the axis of inspection port 1.5; (b) profile along the axis of inspection port 3.6

mated. A possible explanation is the overestimation of soot concentration since, as seen below, the gas species concentrations are in good agreement with the data.

Inspection port 3.6 is located near the front wall and at the top burners level (see Fig. 1(b)). Along the axis of this port the temperature profiles computed using the three grids mentioned above are similar, as shown in Fig. 4(b). The temperature is underpredicted, except in front of the combustion air inlet ( $y \approx 2.4$  m), where a temperature drop is observed due to the stream of relatively cold combustion air. The temperature rises for larger values of  $y$  due to the heat released in the combustion of the fuel injected through the burner closest to port 3.6. There may be several reasons for the temperature underestimation, but first it should be mentioned that this profile is located in a region of steep temperature gradients (see Fig. 3 for small  $x$  values) and very close to the burner inlet. It would be very useful to have temperature measurements along the burner axis, but this is not possible because there is no physical access for the probes.

The burner geometry is rather complex and its details are not taken into account. Due to these limitations, it is not surprising that there is a discrepancy between the data and the predictions for the profile through port 3.6. Apart from the geometry simplifications and the assumptions underlying the combustion model, namely the instantaneous fuel vaporization, other possible explanations for the temperature underprediction may be devised: an overprediction of the heat radiation loss; errors in the as-

sumed relationship between instantaneous values of enthalpy and mixture fraction; and an overestimation of mixture fraction fluctuations. However, much more detailed data would be needed to draw conclusions about the actual reason of the temperature underprediction.

Figure 5 shows the comparison between predicted and measured  $O_2$ ,  $CO_2$ , and  $CO$  mole fractions on a dry basis through inspection ports 1.5 and 2.6. At inspection port 1.5 the predicted  $CO_2$  profiles are grid independent and in good agreement with the data, although there is a slight overprediction of  $CO_2$  mole fraction. The influence of grid refinement can be seen in the predicted  $O_2$  and  $CO$  profiles. Nevertheless, there appears to be a tendency for a slight overprediction of  $CO$  and a slight underprediction of  $O_2$ . The general agreement, however, is rather good.

The mole fractions of  $O_2$ ,  $CO_2$ , and  $CO$  are approximately constant along the axis of inspection port 2.6 up to  $y \approx 1.8$  m, and their values are typical of combustion products that recirculate in this region (see Figs. 5(c) and 5(d)). The presence of  $CO$  with levels between 1 and 2 percent suggests that combustion is not complete. For larger values of  $y$ , a sharp rise of  $O_2$  along with a sudden decrease of  $CO_2$  mole fractions occurs as the stream of combustion air, injected through the burner closest to the injection port 2.6, is approached. As  $y$  increases, the  $O_2$  mole fraction drops and the  $CO$  and  $CO_2$  mole fractions increase, as a result of the combustion phenomena. The  $CO_2$  mole fraction decreases again, as  $y$  increases, up to the axis of the burner, because in front of the burner there is a fuel-rich mixture, and the oxygen mole fraction is zero. The presence of the streams of atomizing air is recognized only if grid 2 is used. This is the grid with the largest number of grid nodes in the burners region. There are no data in the burner region where combustion takes place because droplets of unburned liquid fuel block the probes and prevent measurements from being taken closer to the burner axis.

As far as the species mole fraction profiles though inspection port 2.6 are concerned, it can be seen that the influence of the

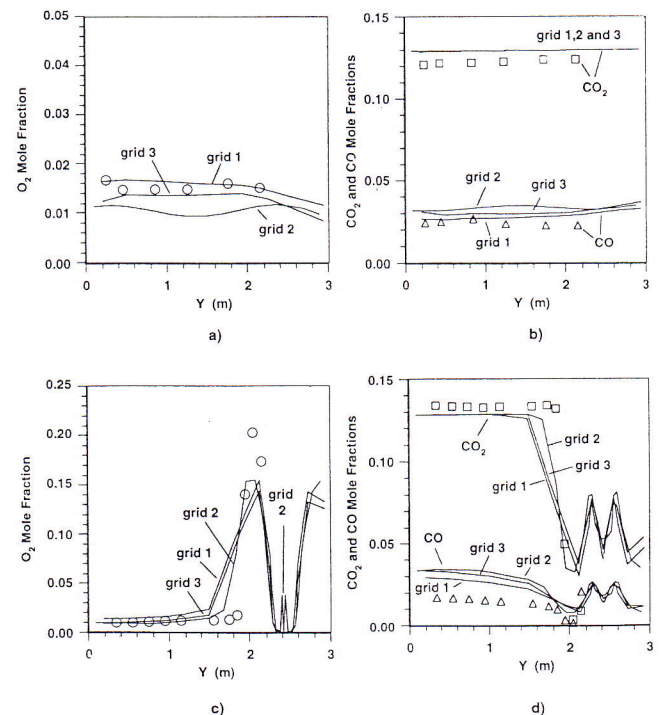


Fig. 5 Comparison between predicted (solid lines) and measured (symbols) mole fraction profiles: (a)  $O_2$  profile along the axis of inspection port 1.5; (b)  $CO_2$  and  $CO$  profiles along the axis of inspection port 1.5; (c)  $O_2$  profile along the axis of inspection port 2.6; (d)  $CO_2$  and  $CO$  profiles along the axis of inspection port 2.6

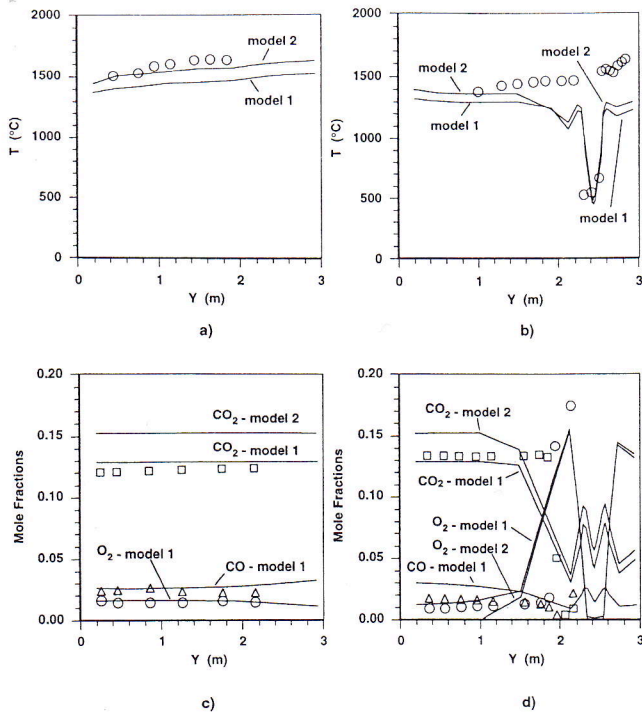


Fig. 6 Comparison between predictions obtained using two different combustion models (model 1: chemical equilibrium; model 2: SCRS; symbols: data): (a) temperature profile through port 1.5; (b) temperature profile through port 3.6; (c) mole fraction profiles through port 1.5. ( $\square$ : CO<sub>2</sub>;  $\Delta$ : CO;  $\circ$ : O<sub>2</sub>); (d) mole fraction profiles through port 2.6. ( $\square$ : CO<sub>2</sub>;  $\Delta$ : CO;  $\circ$ : O<sub>2</sub>)

grid on the predictions is negligible. All the predicted profiles show a good agreement with the data, at least qualitatively. The CO<sub>2</sub> mole fraction is slightly underpredicted up to the burner position. In front of the burner the measured mole fraction decreases rapidly with distance from the burner, whereas the numerical solution exhibits a smoother behavior. However, grid 2 shows a steeper gradient than grids 1 and 3, suggesting that a finer grid along the y direction might improve the results in this region. The predicted O<sub>2</sub> mole fraction is in close agreement with the data up to  $y = 1.5$  m. Farther downstream the rise in O<sub>2</sub> mole fraction is smoother than the data suggest and, once again, the steeper gradient was calculated by grid 2. The peak value of O<sub>2</sub> is underpredicted and this may be attributed to a need for grid refinement. The CO mole fraction is overpredicted but the shape of the profile is in good agreement with the measurements.

The results presented so far show that although it cannot be argued that the results are completely grid independent, it can be concluded that the discrepancies between the data and the predictions are in most cases only explainable by physical reasons or experimental uncertainties. The range of the errors attributable to grid refinement was identified by performing the calculations using three different grids. Therefore, in the following discussion only the results obtained using grid 1 shall be considered.

The influence of the combustion model on the predicted results was investigated by repeating the calculations using the SCRS model instead of the chemical equilibrium model. The results of the two models and the measured values are compared in Fig. 6.

It can be seen that the SCRS yields higher temperature levels. This is an expected result since this model does not take dissociation into account. The SCRS yielded an improvement of the predicted temperature profile through port 1.5 but only marginal improvements were achieved for the profile through port 3.6. However, the gas composition is not adequately predicted by

the SCRS model. In fact, Fig. 6(c) shows that, according to this model, no oxygen is present along the axis of inspection port 1.5. This is not corroborated either by the chemical equilibrium model or by the experimental data. Consequently, the CO<sub>2</sub> mole fraction is significantly overpredicted by the SCRS model. A similar behavior can be seen through port 2.6. Out of the burner region, the SCRS model overpredicted the CO<sub>2</sub> mole fraction and predicted no oxygen. On the other hand, the chemical equilibrium model is in good agreement with the data. Moreover, the SCRS does not take the presence of CO into account.

Hence, it can be concluded that the chemical equilibrium model is preferable to the SCRS model. The reason the SCRS model yielded a better agreement with the measurements for the temperature profile through port 1.5 should not be attributed to its superiority but rather to an overestimated heat loss. This was compensated by the higher temperature calculated when the SCRS model is employed.

**5.2 Influence of the Air/Fuel Ratio.** The effect of decreasing the air/fuel ratio is illustrated in Fig. 7, where the comparison between predicted and measured temperature pro-

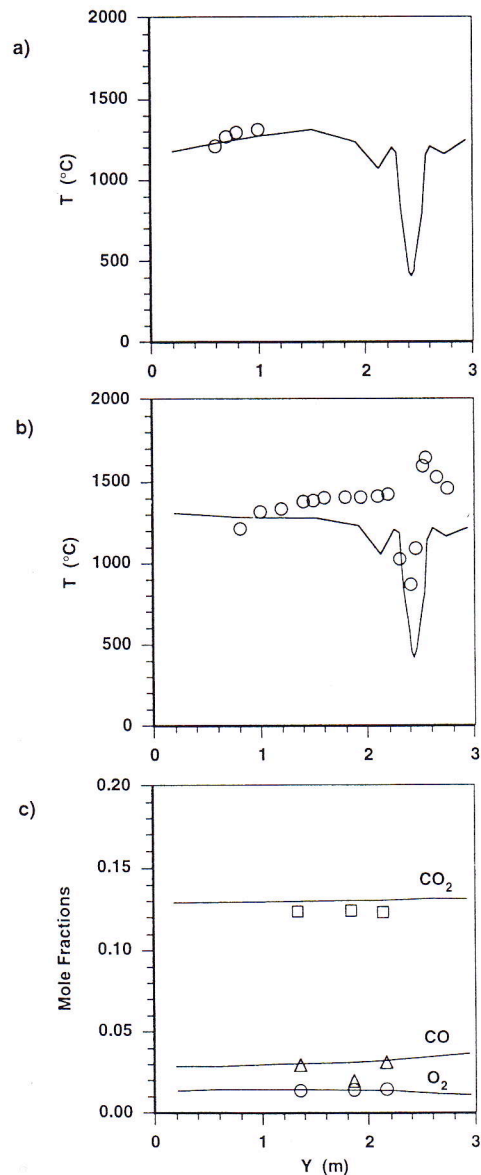


Fig. 7 Comparison between predicted (solid lines) and measured (symbols) for 0.75 percent O<sub>2</sub> in flue gases: (a) temperature profile through port 2.6; (b) temperature profile through port 3.6; (c) mole fraction profiles through port 1.5

files through ports 2.6 and 3.6 and mole fraction profiles through port 1.5 are presented. These results (test case 2) were obtained for a volumetric concentration of  $O_2$  in flue gases of 0.75 percent, whereas at standard operating conditions (test case 1) this concentration is 1.5 percent.

Along the axis of inspection port 2.6, the calculated temperatures are in close agreement with the data, but this is restricted to a small zone out of the flame region. The predicted and measured temperature profiles through port 3.6 are very similar to those presented in Fig. 4(b) for standard operating conditions. The variation in gas temperatures between the two test cases is very small. Nevertheless, the measured gas temperature at the outer side of the flame region is slightly higher for case 1 and this is corroborated by the predictions. The temperature drop observed for  $y \approx 2.4$  m is caused by the stream of combustion air.

The computed mole fractions of  $CO_2$ ,  $CO$ , and  $O_2$  through port 1.5 are in good agreement with the data. The  $CO_2$  mole fraction is about the same for test cases 1 and 2. However, the reduction of the air/fuel ratio yielded a small increase of  $CO$  and a small decrease of  $O_2$  mole fractions. These variations are correctly predicted by the model.

**5.3 Influence of the Boiler Load.** The influence of decreasing the boiler load from 250 MWe (test case 1) to 125 MWe (test case 3) is shown in Fig. 8. The reduction of the boiler load is achieved by turning off the burners of the top level and blocking air access to these burners. However, the blockage is not completely effective and some air escapes through the burners.

The gas temperature through inspection port 1.5 decreases with the power load as both experiments and calculations reveal. The predicted temperature profile for test case 3 is in good agreement with the data, suggesting that, in this case, the radiative heat loss is well predicted. The gas temperature profile along the axis of port 2.6 shows the same kind of discrepancy observed for temperature profiles close to the front wall in other test cases: The temperature is underpredicted except close to the side wall and in front of the combustion air inlet where the temperature falls down. The temperature profile through port 3.6 is rather different because the burners at the third level are out of service. The calculated temperature is constant during the first 2 m and then drops due to the mixture of combustion gases with cold air that escapes through the top level burners. This temperature profile is correctly predicted despite a slight temperature underprediction in the flat temperature region.

## 6 Conclusions

This paper reports the application of a mathematical model to a power station boiler of the Portuguese Electricity Utility. The model is based on the numerical solution of the partial differential equations governing conservation of mass, momentum, energy, and chemical species. The results are compared with measurements recently obtained for several operating conditions.

Calculations were performed using three different grids and a careful analysis was conducted to conclude if the solution was dependent on the grid refinement. The results obtained for standard operating conditions are in good agreement with the available data, except near the burner exit where the temperature is underpredicted. The influence of grid refinement on the predictions is generally negligible, compared with the differences between the numerical solutions and the data, although this is not always the case. Situations where grid refinement might influence the predictions were identified.

The simple chemically reacting system combustion model yields concentrations of the chemical species that disagree with the data. Contrary to the data, according to this model there would be no oxygen close to the side wall. In addition, it did

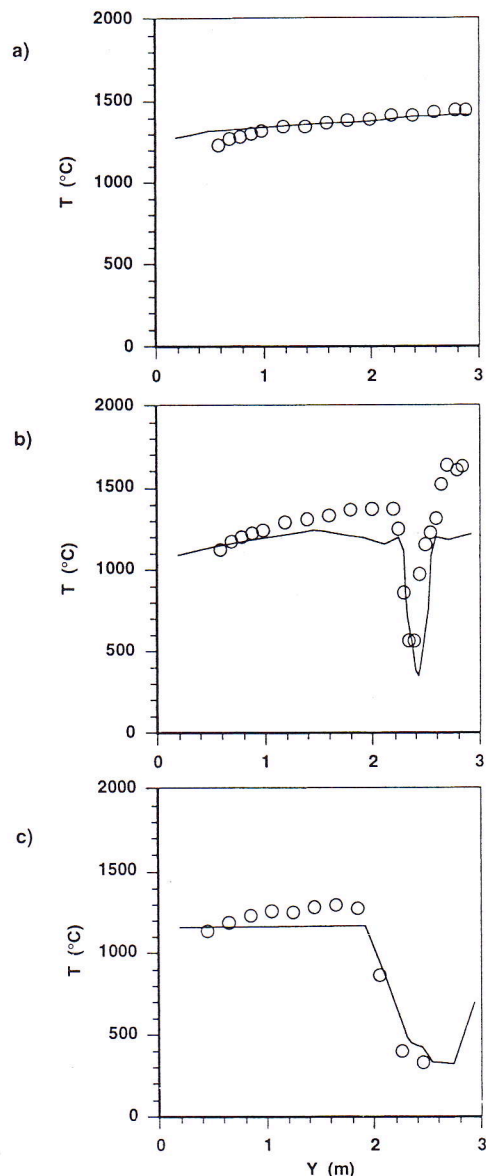


Fig. 8 Comparison between predicted (solid lines) and measured (symbols) temperature profiles at partial load (125 MWe): (a) profile through port 1.5; (b) profile through port 2.6; (c) profile through port 3.6

not take  $CO$  into account. Therefore, the chemical equilibrium model was preferred since it does not suffer from these shortcomings.

The influence of the air/fuel ratio and power load were correctly predicted by the model, demonstrating its ability to perform parametric studies.

The data are restricted to a small number of temperature and chemical species profiles. Moreover, these profiles are located very close to the front and back walls. This is a consequence of the position of inspection ports that provide physical access to the probes. Despite these limitations, this is one of the most complete sets of data for full-scale utility boilers ever reported, and the evaluation reported here has proved the predictive capabilities of the mathematical model, although there is room for further improvements.

## Acknowledgments

This work has been performed within the ESPRIT II European Collaborative Research Programme (Project No. 2192-AIMBURN).

## References

- Abbas, A. S., and Lockwood, F. C., 1986, "Prediction of Power Station Combustors," *21st Symposium (Int.) on Combustion*, The Combustion Institute, pp. 285–292.
- Abou-Ellail, M. M. M., Gosman, A. D., Lockwood, F. C., and Megahed, I. E. A., 1978, "Description and Validation of a Three-Dimensional Procedure for Combustion Chamber Flows," *Journal of Energy*, Vol. 2, No. 2, pp. 71–80.
- Bonvini, M., Piana, C., and Vigevano, L., 1991, "Predictions of Thermal NO<sub>x</sub> Emissions From Utility Boiler Furnaces," *Proc. 1st International Conference on Combustion Technologies for a Clean Environment*, Vilamoura, Portugal, Sept. 3–6, Vol. 2, paper 23.3.
- Boyd, R. K., and Kent, J. H., 1986, "Three-Dimensional Furnace Computer Modelling," *21st Symposium (Int.) on Combustion*, The Combustion Institute, pp. 265–274.
- Butler, B. W., and Webb, B. W., 1991, "Local Temperature and Wall Radiant Heat Flux Measurements in an Industrial Scale Coal Fired Boiler," *Fuel*, Vol. 70, pp. 1457–1464.
- Carvalho, M. G., and Coelho, P. J., 1990, "Numerical Prediction of an Oil-Fired Water-Tube Boiler," *Engineering Computations—Int. J. Computer Aided Engineering and Software*, Vol. 7, No. 3, pp. 227–234.
- Carvalho, M. G., Coelho, P. J., and Costa, F., 1990, "A Comparative Study of the Performance of a Large Industrial Boiler for Fuel Oil and Natural Gas Firing," *Proc. 6th ESPRIT CIM—Europe Annual Conference*, Lisbon, May 15–17.
- Carvalho, M. G., Coelho, P. J., and Costa, F., 1991, "Mathematical Modelling of a Power Station Boiler of the Portuguese Electricity Utility," *Proc. 2nd European Conference on Industrial Furnaces and Boilers*, Vilamoura, Portugal, Apr. 2–5, Vol. 2.
- Cassiano, J., Heitor, M. V., Moreira, A. L. N., and Silva, T. F., 1994, "Temperature, Species and Heat Transfer Characteristics of a 250 MWe Utility Boiler," *Combust. Sci. and Tech.*, Vol. 98, pp. 199–215.
- Coelho, P. J., and Carvalho, M. G., 1992, "Heat Transfer in Power Station Boilers," ASME AES-Vol. 27, R. F. Boehm, ed., New York, pp. 365–372.
- Coimbra, C. F. M., Azevedo, J. L. T., and Carvalho, M. G., 1994, "3-D Numerical Model for Predicting NO<sub>x</sub> Emissions From an Industrial Pulverized Coal Combustor," *Fuel*, Vol. 73, pp. 1128–1134.
- Epple, B., and Schnell, U., 1992, "Modelling and Simulation of Coal Combustion Process in Utility Boiler Furnaces," *Proc. 2nd International Forum on Expert Systems and Computer Simulation in Energy Engineering*, Erlangen, Germany, Mar. 17–20, paper 12-L.
- Fiveland, W. A., and Wessel, R. A., 1988, "Numerical Model for Predicting Performance of Three-Dimensional Pulverized-Fuel Fired Furnaces," ASME JOURNAL OF ENGINEERING FOR GAS TURBINES AND POWER, Vol. 110, pp. 117–126.
- Fiveland, W. A., and Latham, C. E., 1991, "Use of Numerical Modelling in the Design of a Low-NO<sub>x</sub> Burner for Utility Boilers," *Proc. 1st International Conference on Combustion Technologies for a Clean Environment*, Vilamoura, Portugal, Sept. 3–6, Vol. 1, paper 15.1.
- Gillis, P. A., and Smith, P. J., 1990, "An Evaluation of Three-Dimensional Computational Combustion and Fluid-Dynamics for Industrial Furnaces Geometries," *23rd Symposium (Int.) on Combustion*, The Combustion Institute, pp. 981–991.
- Gordon, S., and McBride, B. J., 1971, "Computer Program for Calculation of Complex Equilibrium Composition, Rocket Performance, Incident and Reflected Shocks and Chapman–Jouguet Detonations," NASA SP-273.
- Görner, K., and Zinser, W., 1988, "Prediction of Three-Dimensional Flows in Utility Boiler Furnaces and Comparison With Experiments," *Combust. Sci. and Tech.*, Vol. 58, pp. 43–58.
- Hottel, H. C., and Sarofim, A. F., 1967, *Radiative Transfer*, McGraw-Hill, New York.
- Jones, W. P., and Whitelaw, J. H., 1982, "Calculation Methods for Reacting Turbulent Flows: a Review," *Combustion and Flame*, Vol. 48, pp. 1–26.
- Khan, I. M., and Greeves, G. A., 1974, "A Method for Calculating the Formation and Combustion of Soot in Diesel Engines," in: *Heat Transfer in Flames*, Afgan, and Beer, eds., pp. 391–402.
- Lauder, B. E., and Spalding, D. B., 1974, "The Numerical Computation of Turbulent Flows," *Comput. Methods Appl. Mech. Eng.*, Vol. 3, pp. 269–289.
- Lockwood, F. C., and Naguib, A. S., 1975, "The Prediction of the Fluctuations in the Properties of Free, Round-Jet, Turbulent, Diffusion Flames," *Combustion and Flame*, Vol. 24, pp. 109–124.
- Lockwood, F. C., and Shah, N. G., 1981, "A New Radiation Solution Method for Incorporation in General Combustion Prediction Procedures," *18th Symposium (Int.) on Combustion*, The Combustion Institute, pp. 1405–1414.
- Lockwood, F. C., Papadopoulos, C., and Abbas, A. S., 1988, "Prediction of a Corner-Fired Station Combustor," *Combust. Sci. and Tech.*, Vol. 58, pp. 5–24.
- Luo, X.-L., Boyd, R. K., and Kent, J. H., 1991, "Computational Investigation of Burnout in a Furnace Firing Pulverized Coal," *J. Institute of Energy*, Vol. 64, Dec., pp. 230–238.
- Magnussen, B. F., and Hjertager, B. H., 1977, "On Mathematical Modelling of Turbulent Combustion With Special Emphasis on Soot Formation and Combustion," *16th Symposium (Int.) on Combustion*, The Combustion Institute, pp. 719–728.
- Robinson, G. F., 1985, "A Three-Dimensional Analytical Model of a Large Tangentially Fired Furnace," *J. Institute of Energy*, Sept., pp. 116–150.
- Sargianos, N. P., Anagnostopoulos, J., and Bergeles, G., 1990, "A Numerical Algorithm for Gas Combustion in Utility Boilers," in: *Advanced Computational Methods in Heat Transfer*, L. C. Wrobel, C. A. Brebbia, and A. J. Novak, eds., Springer-Verlag, Vol. 3, pp. 155–170.
- Truelove, J. S., 1976, "A Mixed Grey Gas Model for Flame Radiation," AERE Harwell, Report HL76/3448/KE.